International Journal of Science and Research (IJSR)
ISSN (Online): 2319-7064
Index Copernicus Value (2015): 78.96 | Impact Factor (2015): 6.391

Effect of Graphene Oxide on Mechanical and Thermal Properties of Polypropylene Nanocomposites

Daniel N. Njoroge

Department of Mechanical and Manufacturing Engineering, Aalborg University, Fibigerstraede 16, DK-9220 Aalborg East, Denmark

Abstract: ***In this study, modified-graphene oxide/polypropylene nanocomposites with varying nanofiller concentrations were prepared, their mechanical and thermal properties characterized i.e. strength, viscoelasticity, crystallinity and toughness properties. The results indicate modified-graphene oxide on isotactic polypropylene had different directional trends. Neat isotactic polypropylene displayed superior properties to isotactic polypropylene nanocomposites in Young's modulus, elongation at break and toughness. On the other hand, isotactic polypropylene nanocomposites displayed enhanced properties to neat isotactic polypropylene in tensile strength (≈ 1.6%), storage modulus (≈ 25%), loss modulus (≈ 15%) and crystallinity (≈ 15%). The enhancement of mechanical properties in isotactic polypropylene nanocomposites in this work is attributed to the high specific surface area of reduced graphene oxide sheets and their better dispersion in polymeric matrix as confirmed using light microscopy.***

Keywords: Graphene oxide, Polypropylene nanocomposites, Mechanical properties, Thermal properties

1. Introduction

Graphite is a cheap and naturally existing material, composed of stacked 2D graphene layers that are held together by van der Waals forces. The introduction of graphite or its modified form as a filler in polymer matrix improves their mechanical, thermal, electrical and barrier properties, hence the popularity of graphitic nanocomposites subject among researchers. In this study, modified graphite was used in the processing of graphene nanocomposites. Graphene is a potential replacement of other graphitic carbon compounds, such as carbon nanotubes (CNTs) in many application. Graphite resource is abundant and its processing approaches are cheaper and more convenient unlike the latter which utilize expensive equipment and high energy processes [1, 2].

Graphitic nanocomposites have been investigated by various researchers. Superior properties have been reported for graphitic nanocomposites in comparison to the non-graphitic-composites. Graphene in nanocomposites is utilized at very low volume fractions but with remarkable property enhancement. In addition, cheap approaches to produce graphene and more importantly in large scale have been reported widely. This has developed interest in graphene nanocomposites area. However, these nanocomposites cannot match the mechanical strength of CNTs because of their stronger entanglements [3]. Graphite is one of the stiffest materials in nature with an elastic modulus of over 1 TPa [4]. Graphite can be processed as either a monolayer graphene sheet, graphene nanoplatelets (GNPs) or graphene oxide (GO), for utilization as 2D nanofillers in polymer nanocomposites.

The chemical conversion of graphite to GO is an approach that avails graphene-oxide sheets in adequate quantities for mass production. This is a primary advantage over the monolayer graphene sheet approaches which have low yields but high quality 2D sheets [5]. Pristine graphene has superior mechanical properties, thus their inclusions in polymeric materials strengthens their structural framework. However, pristine graphene has a tendency to agglomerate in polymeric based materials due to its non-reactive nature that results to poor mechanical properties. Therefore, its reactivity is increased through oxidation and chemical surface modification which opens up reactive sites that it could bond with the chemical agent and to the polymer matrix. This undoubtedly produces an improved graphene dispersion as compared to the latter, hence remarkable mechanical properties [1]. Therefore, the modification of the filler surface by coupling agents improves their dispersibility in polymer matrix. Here-in maleic anhydride grafted polypropylene was used as a compatibilizer in the processing of polypropylene nanocomposites. The couplant therefore, lowers the cohesive forces between the nanoparticles and enhances their compatibility with the polymer thus improving the dispersion phenomenon. Moreover, OFGs in graphene oxide can react on their surfaces with monomers to form covalently bonded nanocomposites. Such bonds have been reported to assist in better dispersion of the filler in polymeric matrices [6]. Here-in, the graphene oxide was functionalized with octadecylamine to form covalent bonds with the carboxylic groups in graphene oxide [7].

Graphene-based nanofiller materials derived from GO and their inclusion in polymer matrix are of recent origin unlike the polymer/GNP nanocomposites which have been the main research focus for several decades. GO-derived fillers have high property enhancement compared to GNPs fillers in polymer nanocomposites. This is influenced by the thin layers which have high surface areas. GO-derived fillers exhibit high electrical conductivity, high moduli and can be easily functionalized to tailor their compatibility with a particular polymer matrix [4].

One major challenge in processing nanocomposites is the dispersion and distribution of fillers. Inadequate dispersion

compromises surface area where the aggregates act as defects which compromise the properties of the nanocomposites. Distribution defines the homogeneity of the filler in the sample whereas the dispersion defines the level of agglomeration [8].

The most useful mechanical properties of polymer nanocomposites are strength, Young's modulus, toughness and elasticity. These properties are related to dispersion quality of nanofillers in the polymer matrix [1]. A uniform dispersion may aid in load transfer in the nanocomposites with few structural flaws which lower their mechanical performance. The dispersion quality have been reported as a dependency of nanocomposites mechanical properties by many researchers. However, the dispersion quality decreases with high content of nanofillers, which is caused by increase in agglomeration tendency [1, 9]. This study analyses the quality of mechanical properties enhancement due to graphene inclusions on isotactic polypropylene (iPP) matrix.

Thermal behavior are the changes that take place in a material upon heating and cooling. Polymer nanocomposites exhibit three main transitions during heating and cooling i.e glass transition, crystallization and melting. Here-in, the transitions on the nanocomposites were also studied and compared to the pure polymer.

2. Materials and Methods

2.1 Materials

Isotactic polypropylene homopolymer (iPP, HE365FB, MW = 230 000 g/mol., melt flow index determined by ISO 1133 method: 12 g/10 min) was obtained from Borealis (Austria) and maleic anhydride grafted polypropylene (MAPP) compatibilizer (G-3015) was obtained from Eastman (USA). Octadecylamine ($C_{18}H_{39}N$, ODA, MW = 269.52 g/mol) was procured from Merch Schuchard (Germany). Hydrazine hydrate (35% soln. in H_2O, grade 98\%) and Hydrogen peroxide (H_2O_2) were procured from Sigma Aldrich (Germany). Natural Graphite (NG), Sulphuric acid (H_2SO_4), Nitric acid (HNO_3), Potassium permanganate ($KMnO_4$) and Toluene (C_7H_8) were available in the polymer processing laboratory. Other agents used were of analytical grade and all solutions were prepared with deionized water.

2.2 Preparation of Graphene Oxide

The oxidation of NG was done using a modified Hummers' method. Typically the preparation process included: 100 mL of H_2SO_4 was mixed with 16.5 mL of HNO_3, in a 250 mL beaker inside an ice bath and the mixture was maintained under constant magnetic stirring. 2.42 g of NG was added to the mixture which turned black in color as stirring was continued for 30 min. 15 g of $KMnO_4$ was gradually added (in $\approx 15\ min$) to avoid overheating and temperature was maintained below $10°C$. A dark green suspension was formed. The mixture was then heated to $35°C$ and held for 1 h. The viscosity of the mixture increased with time resulting to a thick suspension. Deionized water was then added gradually to the mixture until the 250 mL beaker was full. The temperature was then raised to $98°C$ and maintained for 2 h. The reaction was terminated by adding the beaker contents on to a larger beaker which contained 280 mL deionized water. 10 mL of H_2O_2 was added gradually with continued stirring to reduce unreacted oxidant and the suspension turned brownish. The suspension was then filtered using a vacuum assisted filtration system to obtain the GO powder. The filter system contained a standard filter paper (HVLP, 0.45 µm resting on top of porous disc. The GO powder obtained on the filter paper was washed with 10 % HCL to remove sulphates present and filtered through the vacuum system. Subsequently, it was washed with ethanol and water to remove other impurities and acids. This washing achieved an equivalent pH compared to that of deionized water used in this study (i.e. pH=5). The obtained GO powder was noted as GO.

2.3 Functionalization of GO using ODA

Chemical functionalization of GO was done using ODA. According to a modified-recipe reported by Bao [10] and Wang, Shen [11], GO was functionalized as follows: ODA solution was prepared by dissolving 0.010 moles of ODA (1.5 g) in ethanol (150 mL) at room temperature, then magnetically stirred for 30 min. 1 g of GO powder was dispersed in 250 mL of ethanol to achieve a nominal concentration of 4.0 mg/mL. The ODA solution was then added into the GO suspension and the mixture was refluxed at $100°C$ for 24 h under constant magnetic stirring. During the ODA functionalization, the color of the GO solution gradually changed from yellow to black. This change indicated a significant chemical change through functionalization [12]. The GO-ODA suspension obtained was noted as functionalized GO (fGO).

2.4 Reduction of fGO

The reduction process was performed using hydrazine hydrate. Typically, 3.75 mL of hydrazine hydrate was added into GO-ODA suspension (fGO) and the mixture refluxed at $100°C$ for 24 h under constant magnetic stirring. Then, the suspension was vacuum filtered and washed thoroughly using ethanol and water to remove any entrapped or unreacted ODA and hydrazine respectively, and GO powder was obtained. The GO powder was dried in the air oven at $110°C$ for 24 h to obtain dry GO powder which was noted as r-fGO.

2.5 Preparation of Nanocomposites

Three types of iPP nanocomposites were prepared by varying filler weight compositions at: 0, 1 and 5% to examine their reinforcing effects accordingly. The nanocomposites were prepared thermally through compounding and injection molding processes respectively. Hygroscopic polymers can result in major molding problems if absorbed moisture is not removed prior to molding. Defects and losses in physical properties are the most common outcomes [13]. Therefore, MAPP and iPP were dried using a vacuum oven (VT6130, Heraeus Vacutherm) at $110°C$ for 24 h to adjust the moisture content to 1-3% and then stored in sealed polyethylene bags.

2.5.1 Compounding

Typically, the compounding procedure included: Blends were prepared by varying filler weight compositions at: 0, 1 and 5%. Based on the total weight of iPP and r-fGO, 5 wt.% MAPP compatibilizer was added to the blend. The r-fGO was dispersed in ethanol (50 mL) in a 250 mL beaker. Both iPP and MAPP were then added to the suspension. The mixture was stirred using a mechanical stirrer by hand for 10 min then poured into an aluminum pan and finally dried using an air oven at $100℃$ for 24 h to get rid of the ethanol. After drying, the modified GO was left embedded on to the blends surfaces in an even fashion. The blends were then fed in to a micro-compounder (MC 15 cc, Xplore Instruments) consisting of a twin-screw extruder. The melt compounding temperature was set to $175℃$, screw speed at 60 rpm and compounded at 5, 10 and 20 minutes. The compounding conditions used have been reported as most convenient in processing polypropylene nanocomposites [14]. The r-fGO/iPP nanocomposites had an extruder residence time of 60 seconds. The extruded strands were then air cooled at ambient temperature before being pelletized using a rotating cutter. The pellets were then stored in sealed polyethylene bags to prevent moisture absorption from the surroundings.

2.5.2 Injection Molding

e r-fGO/iPP nanocomposites test samples were prepared using a piston injection moulding machine (Thermo Scientific HAAKE MiniJet II). The injection molding conditions used in this study are shown in Table I. These molding conditions are based on the authors' trial experiments, previous studies done by other researchers on poly-propylene polymer [15] and technical data sheets of the materials used [16, 17]. The pellets were then charged in the injection cylinder and the r-fGO/iPP nanocomposites test samples were injection molded at $220℃$.

Table 1: Injection molding conditions for IPP nanocomposites

Condition	Setting
Injection pressure	600 bar
Injection Temperature	$220℃$
Injection Time	20 s
Mold Temperature	$30℃$
Cooling Time	20 s

2.6 Characterization

2.6.1 Characterization of GO, fGO and r-fGO

GO, fGO and r-fGO were characterized using a solubility test. The test was done at room temperature ($\approx 25℃$). Dried samples were dispersed in toluene at a concentration of 3.0 mg/mL, bath sonicated for 10 min and allowed to settle for 1 h. The dispersion phenomena of the dried samples in the non-polar solvent was used to determine the success of modification of the GO to fGO and finally to r-fGO.

2.6.2 Tensile Properties Measurements

The nanocomposites test samples were prepared through micro-compounding and injection molding. Dogbone shaped samples of $4.2 \times 2.0\ mm$ in width and thickness respectively were used. The test was done using the Zwick tensile testing machine (Z100) as per ISO 527-2 Standard [18] at room temperature. A 5 KN tensile load cell with a tensile speed of 20 mm/min was used for all tests. The tensile strength, Young's modulus and elongation at break of the nanocomposites were measured. Average tensile properties of 5 nanocomposite specimens was reported for all series.

2.6.3 DMA Measurements

DMA analysis was conducted on iPP nanocomposite specimens using TA 8000 DMA analyzer in argon atmosphere. Injection molded specimens of $50 \times 9.8 \times 3.2\ mm$ were used in the three point bend test according to ISO 178 standard [19]. After specimen calibration, the samples were loaded in the fixtures and subjected to a heating rate of $3℃/min$ in the heating range of $30 - 100℃$. The test was carried out at a constant frequency of 1 Hz with an amplitude of 100 µm. The tests were repeated three times for Neat iPP samples (S-0-0) to check for consistency of results. For all other series, only one sample was tested.

2.6.4 DSC Measurements

DSC analysis was performed on iPP nanocomposites specimens using TA Q2000 DSC analyzer in nitrogen atmosphere. Samples were ground using a rotary grinder to reduce the thickness to $\approx 1\ mm$. Film samples of $\approx 10\ mg$ by weight were cut from the ground specimens using a punch plier. The films were then placed in sealed cells and subjected to a heat/cool/heat cycle. The three cycles included: Initial heating rate of $10℃/min$, followed by a slow cooling rate of $5℃/min$ and a final heating rate of $10℃/min$. All heat and cool cycles were performed in the temperature range of $-20 - 200℃$. The degree of crystallinity, χ_c was determined using (1).

$$\chi_c = \frac{\Delta H_m^{Norm}}{\Delta H_m^{\circ}} \quad (1)$$

where $\Delta \boldsymbol{H_m^{Norm}}$ is the calculated normalized heat of fusion (melting) and $\Delta \boldsymbol{H_m^{\circ}}$ is the heat of fusion of an ideal 100 % crystalline material [20, 21]. $\Delta \boldsymbol{H_m^{Norm}}$ was determined according to (2);

$$\Delta H_m^{Norm} = \frac{\Delta H_m}{wt\%_{iPP}} \quad (2)$$

where ΔH_m is the experimentally observed heat of melting and $wt\%_{iPP}$ is the weight fraction of iPP in the nanocomposite. The pure crystalline iPP has a value of $\Delta H_m^{\circ} = 209\ J/g$ [20], which was used in calculating the χ_c for the neat iPP and its nanocomposites. One sample was tested for each series.

2.6.5 IZOD Impact Test

The unnotched impact test specimens obtained through compounding and injection molding of $79 \times 9.8 \times 3.2\ mm$ in size were held on the clamp with a torque of 5 Nm. The test was conducted at an impact velocity of 3.5 m/s with a 50 J hammer on a pendulum impact tester (CEAST 9050, Instron) at room temperature ($25℃$) in accordance with ISO standard 180 [22]. Three samples were tested for every series.

2.6.6 Light Microscopy Study

Paraffin samples of 55 µm thickness were trimmed from rectangular specimens ($9.8 \times 3.2\ mm$) using a Microtome

(Leica RM2145). The paraffin samples were placed on glass slides and observed under a light microscope (Zeiss) using X5 magnification objective lens.

3. Results and Discussion

3.1 Dispersion of GO, fGO and r-fGO

GO is polar thus it completely disperses in polar solvents such as H_2O. On the other hand, it has low dispersion in non-polar solvents, due to the presence of high number of polar OFGs on its surfaces [23]. The functionalization of GO with ODA makes the hydrophilic GO hydrophobic. This increases its dispersibility in non-polar solvents because of the grafting of the long octadecyl chain on GO. Therefore, GO, fGO and r-fGO were dispersed in toluene which is a non-polar solvent at a concentration of 3.0 mg/mL, bath sonicated for 10 min and allowed to settle for 1 h. Figure 1(a-c) shows the distinct solubility of GO, fGO and r-fGO in toluene solvent. The fGO and r-fGO displayed excellent dispersibility in toluene solvent. On the other hand, GO settled at the bottom of the beaker, thus displaying very poor dispersion in toluene solvent. This is attributed to the incompatibility of GO and toluene; GO is polar while toluene is non-polar. Figure 1(d) shows the complete dispersion of GO in H_2O (polar solvent). The results therefore indicate successful conversion of hydrophilic GO to a hydrophobic state (fGO) after refluxing with ODA. This hydrophobic nature will necessitate good dispersion of modified GO and enhance its interfacial interaction with non-polar polymers [24], such as iPP that is utilised in this study.

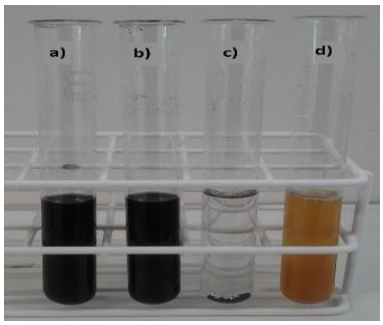

Figure 1: Dispersion of: (a) r-fGO, (b) fGO, (c) GO in toluene and (d) GO in water.

3.2 Tensile Properties

The tensile properties of the nanocomposites determined are tensile strength, Young's modulus and elongation at break. In general, the Young's modulus and the elongation at break of neat iPP were higher than that of iPP nanocomposites, an indication of stiffer and extremely tough matrix in comparison to all modified-GO reinforced nanocomposites. 5% GO nanocomposites displayed a higher elongation at break than 1% GO category. On the contrary, 1% GO nanocomposites had higher a Young's modulus than the 5% category.

On the other hand, iPP nanocomposites registered comparable and even higher values of tensile strength than neat iPP. 5% GO nanocomposites indicated the highest tensile strength among all the series tested, whereas the 1% GO category showed a lower and comparable strength as the neat iPP.

The interpretation therefore; increasing GO content from 1% to 5% caused an increase in tensile strength and elongation at break in iPP nanocomposites which is supported by experimental results shown in Figure 2 and 3 respectively. In addition, an intermediate compounding time of 10 min registered the peak values for tensile strength and elongation at break.

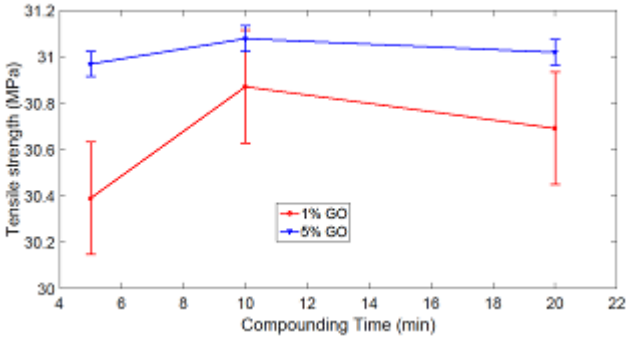

Figure 2: Tensile strength of iPP nanocomposites with varying compounding time.

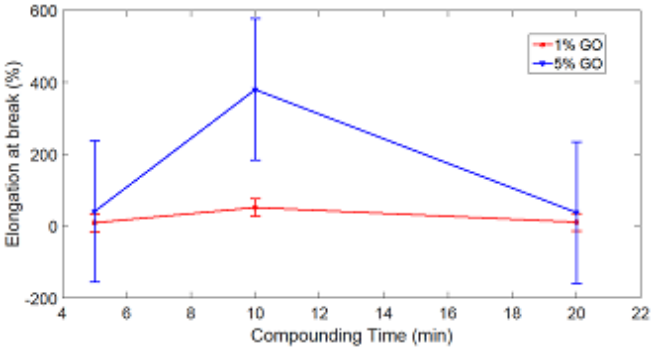

Figure 1: Elongation at break of iPP nanocomposites with varying compounding time.

On the other hand, the Young's modulus had a completely different trend as shown in Figure 4. Increasing GO content from 1% to 5% caused a decrease in Young's modulus at lower compounding time. Consequentially, this trend was reversed at 11 min mark (near to 10 min compounding time), hence higher filler nanocomposites registered higher Young's modulus at high compounding time.

The enhancement of tensile strength with the increase of nanofiller loading shows a better compatibility of iPP matrix filled with modified-GO. This phenomena shows the reinforcing effect of GO as a filler in polymer nanocomposites. A similar increasing trend has been reported by other researchers in the case of other carbon filled polypropylene systems [25].

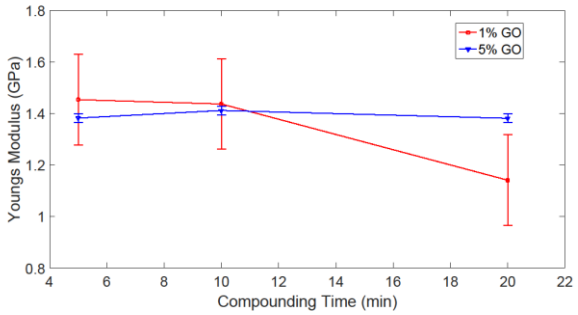

Figure 2: Young's modulus of iPP nanocomposites with varying compounding time

The elongation at break of nanocomposites was greatly reduced in comparison to the neat iPP. This is an indication of increasing degree of brittleness with addition of GO content. The GO crosslinks with the matrix, hence hindering the movement of polymer chains. The elongation at break was enhanced by increasing GO content from 1% to 5% although this was way-below the performance of the neat iPP. This decreasing trend in comparison to neat iPP has been reported by other researchers in the case of other carbon based PP systems [25].

The Young's modulus of nanocomposites was reduced in comparison to the neat iPP. The Young's modulus was higher in 1% GO iPP nanocomposites than in 5% GO nanocomposites. This is an indication that 1% GO iPP nanocomposites had better physical crosslinking between the polymer and GO resulting in a stiffer structure than the 5% GO nanocomposites. Contrary to the expectation, the Young's modulus was not enhanced by the increasing GO content from 1% to 5%. The observed phenomenon may explain ineffective GO dispersion in iPP nanocomposites which may have caused agglomeration of reinforcing fillers at high GO content (5%) thus reduced stiffness properties.

The compounding time was also found to influence the tensile strength, Young's modulus and elongation at break properties. Short (5 min) and long (20 min) compounding times displayed inferior tensile strength, Young's modulus and elongation at break properties. Intermediate compounding time (10 min) gave enhanced and balanced properties.

The observed trend could be explained by ineffective GO dispersion during short and long compounding times, causing GO agglomeration, thus poor nanocomposite performance. On the other hand, intermediate compounding time may have resulted to better GO dispersion hence the enhanced properties. Good dispersion of reinforcing fillers have been reported to enhance nanocomposite properties [4].

3.3 DMA Analysis

The DMA experiment was used to study the viscoelastic properties of neat iPP and iPP nanocomposites. The change in storage modulus (E') and loss modulus (E") was recorded as a function of temperature during heating under argon gas. Figure 5 and 6 shows the effect of GO content on storage and loss modulus respectively, for neat iPP and iPP nanocomposites at 5 min compounding time.

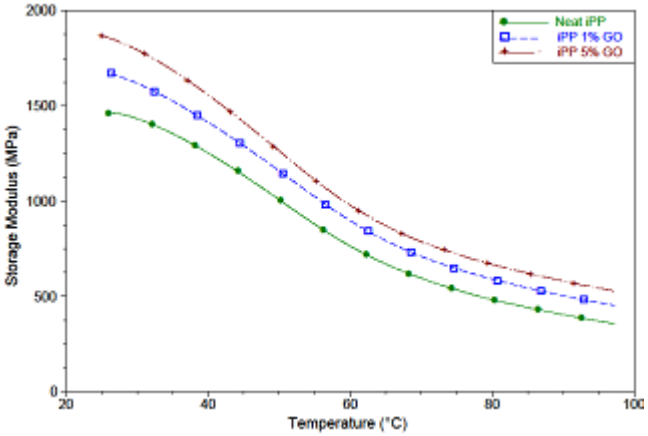

Figure 3: Effect of GO content on storage modulus for iPP nanocomposites at 5 minutes compounding time.

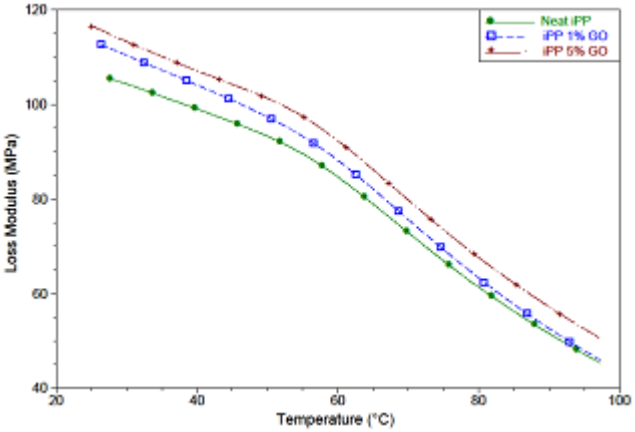

Figure 4: Effect of GO content on loss modulus for iPP nanocomposites at 5 minutes compounding time.

From the above figures, the trend in all samples was an enhancement of storage and loss modulus with increase in GO content in the whole temperature range, in comparison to the neat iPP. The moduli trend order was: iPP 5% GO > iPP 1% GO > neat iPP. This behavior was similar in all the other compounding times i.e 10 and 20 min. The increase in moduli with increasing GO content found in this study may be attributed to the increasing degree of crosslinking. Increasing GO content results to additional crosslinking between GO particles and the polymer matrix, resulting to less mobility of the sub-chains in the polymer nanocomposite network which was confirmed in the tensile analysis.

A similar trend of moduli has been reported in the case of other GO filled polymer nanocomposites [25].

The compounding time was also found to have an influence on the moduli. Figure 7 and 8 shows the effect of compounding time on storage and loss modulus respectively, for iPP nanocomposites.

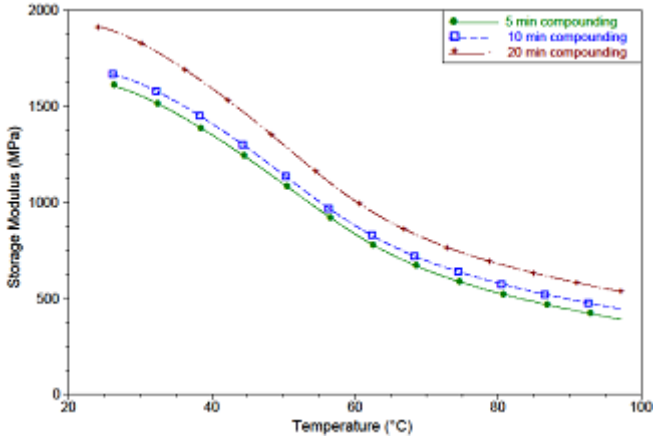

Figure 5: Effect of compounding time on storage modulus for 1% GO filled nanocomposites.

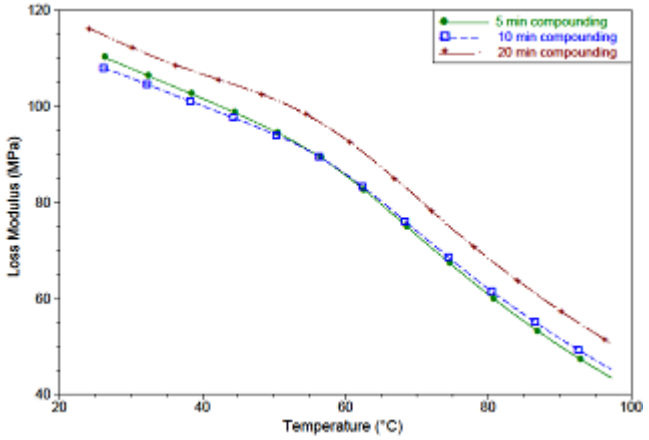

Figure 6: Effect of compounding time on loss modulus for 1% GO filled nanocomposites

From the above figures, the trend in all samples was an enhancement of the storage and loss modulus with increase in compounding time in the whole temperature range. The moduli trend order was: 20 > 10 > 5 min compounding time. This behavior was similar in 5% GO filled nanocomposites. The increase in moduli with increasing compounding time found in this study may be attributed to decreasing dispersion quality. At high compounding time, the melt becomes more fluid during compounding which causes a drop in shearing force. As a result, the dispersion quality is reduced which causes GO agglomeration hence increased stiffness. A similar trend of moduli has been reported in the case of other filler iPP nanocomposites [26].

3.4 DSC Analysis

Melting transitions were identified in the first cycle (1st heating) and third cycle (2nd heating). The heat of melting and melting temperature of polymers and their nanocomposites are influenced by thermal history applied during processing [27]. More heat was consumed in melting the neat iPP and its nanocomposites in the 2nd heating compared to the 1st heating. The 1st heating cycle gives the actual state of the material crystals after processing (disordered state). The slow cooling cycle erases the previous thermal history on the material (ordering phase) and imparts a known thermal profile upon it [28], which is revealed in the 2nd heating cycle. Therefore, the inherent melting transition of the neat iPP and its nanocomposites were evaluated using the third cycle (second heating). In addition, neat iPP and its nanocomposites had higher melting temperatures in the 1st heating in comparison to the 2nd heating. Increasing GO content from 1% to 5%, increased the melting temperature of the iPP nanocomposites. A similar trend on melting temperature has been reported [29]. This trend can be explained by the un-plasticizing effect of the GO.

The degree of crystallinity, χ_c of neat iPP and its nanocomposites was also analysed. The values in the 1st heating cycle had a decreasing trend, which represent the state of the material (thermal history). In contrast, the 2nd heating cycle had a consistency increasing trend, which represent the *true initial crystallinity*. The crystallinity increased in all samples with increase in GO content. The χ_c trend order was: iPP 5% GO > iPP 1% GO > neat iPP.

The compounding time was also found to influence the χ_c. The χ_c increased in all samples with increase in compounding time. The χ_c trend order was: 20 > 10 > 5 min compounding time. A similar trend of χ_c has been reported in the case of expanded graphite [20] and GO [24] filled nanocomposites. These crystallinity trends may explain the higher tensile strength and elongation at break of 5% GO filled nanocomposites compared to 1% GO nanocomposites, which is attributed to enhanced interaction between the modified GO and iPP.

Here-in, the glass transition was not revealed in all the DSC scans for neat iPP and its nanocomposites. The DSC scans were carried out with a lower boundary temperature of $-20°C$. Therefore, the glass transition was expected as several sources indicated a T_g between $0 - 20°C$ [30]. These results therefore indicate the possibility of a T_g value below $-20°C$.

Figure 9 and 10 shows the crystallization behavior of neat iPP and its nanocomposites. This transition was identified in the second cycle where the melt was cooled from 200 to $-20°C$ after the first heating cycle. The crystallization temperature of neat iPP was $\approx 8°C$ lower than all iPP nanocomposites tested. The modified GO clearly acted as a nucleating agent for the crystallization of iPP matrix. Many researchers who have studied inclusion of fillers in iPP nanocomposites, reported initiated crystallization at higher temperatures because the fillers acted as nucleating agents [20]. The crystallization temperatures for 1% GO filled iPP nanocomposites was $\approx 123°C$, whereas 5% GO filled iPP nanocomposites was $\approx 124°C$. Therefore, these results show a slight change in nucleation effect by increasing the GO content from 1% to 5%. A similar trend has been previously reported [25]. The inferior increment in nucleating ability can be explained by the low variation in GO surface area for adsorption of the iPP chain [29]. To register a significant change in nucleation effect, a high variation in GO surface area may be required. This may explain why the crystallinity values for 5% GO filled iPP nanocomposites showed a similar trend (slight increase) in crystallinity when GO content was increased from 1% to 5%.

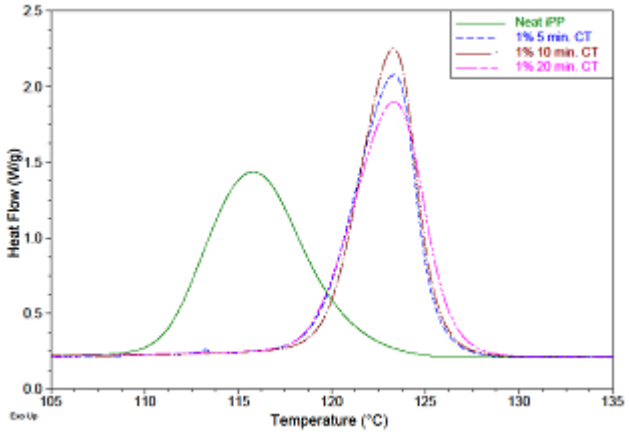

Figure 7: Effect of GO content on crystallization behavior for neat iPP and 1% GO filled nanocomposites.

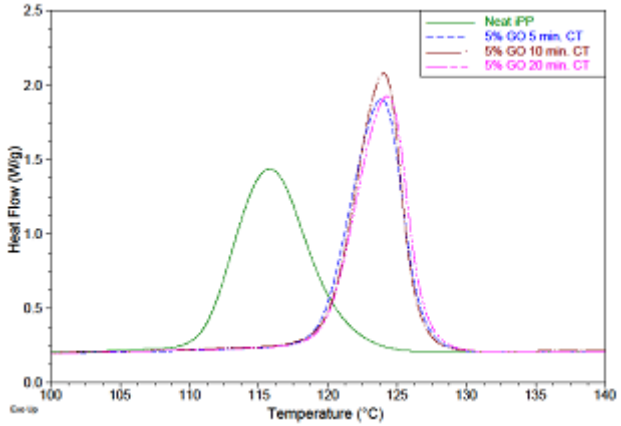

Figure 8: Effect of GO content on crystallization behavior for neat iPP and 5% GO filled nanocomposites.

3.5 Izod Impact Strength

The IZOD impact test was used to measure the energy consumption of neat iPP and iPP nanocomposites during the impact process. All specimens failed in one blow using the 50 J hammer released from $150°$ position. All samples failed in one mode: a complete break into two pieces, implying their brittle nature.

The impact strength trends of the iPP nanocomposites are shown in Figure 11. This plot represents the mean impact strength values of all the series with relative deviation. The mean impact strength of neat iPP was $\approx 1.2\ KJ/m^2$ which was lower than for all iPP nanocomposites tested, an indication of a toughening mechanism by the modified-GO particles in the matrix. 5% GO nanocomposites displayed a higher impact strength than 1% category on low and intermediate compounding times. On high compounding time, 5% GO nanocomposites displayed lower impact strength.

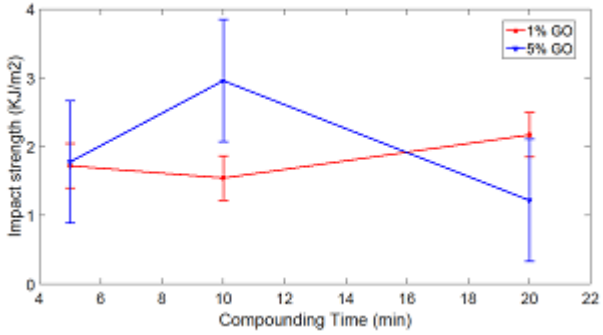

Figure 9: Impact strength of iPP nanocomposites with varying compounding time.

Increasing GO content from 1% to 5% caused a slight increase in impact strength. An intermediate compounding time of 10 min registered the peak values for impact strength. Consequentially, this trend was reversed at high compounding time, hence higher filler nanocomposites registered lower impact strength at high compounding time of 20 min. The enhancement of impact strength with the increase of GO, shows compatibility of iPP matrix with the GO as well as the reinforcing effect of GO as a filler in polymer nanocomposites. Similar trends has been reported by other researchers [31].

Figure 12 and 13 shows the force-time plots for the impact test. The test specimens are abbreviated as shown in Table 2. The impact forces increase up to a maximum value and then quickly drops, implying that high energy is used up in the crack initiation stage while propagation and crack growth consumes little energy. From the results, neat iPP consumed more energy in breakage than all iPP nanocomposites tested. This is an indication that neat iPP it tougher than its nanocomposites. Figure 14 shows the effects of increasing GO content from 1% to 5%. The amount of fracture energy (area under the curve) is reduced. This is an indication that the material becomes more brittle with increase in GO content. Therefore, the addition of GO to iPP matrix compromised its toughness. Similar scenarios have been reported on many nanocomposites impact tests [31].

Table 2: Abbreviation of test specimens

Specimen Identifier	Series
Neat iPP	S-0-0
1% 5 min	S-1-5
1% 10 min	S-1-10
1% 20 min	S-1-20
5% 5 min	S-5-5
5% 10 min	S-5-10
5% 20 min	S-5-20

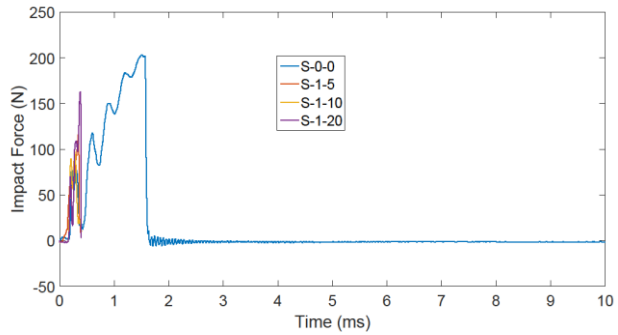

Figure 10: Force-time plots for neat iPP and 1% GO filled nanocomposites.

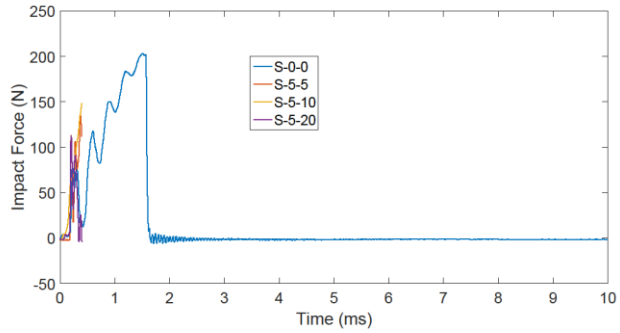

Figure 11: Force-time plots for neat iPP and 5% GO filled nanocomposites.

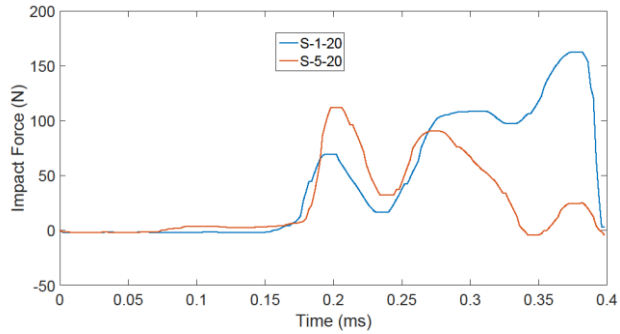

Figure 12: Force-time plots for 1% and 5% GO filled nanocomposites.

3.6 Light Microscopy Analysis

The dispersion state of modified GO on iPP nanocomposites was studied using light microscopy. A low magnification of X5 was selected in order to characterize the state of dispersion. The dispersion micrographs of 1 wt.% and 5 wt.% modified GO filled iPP nanocomposites are shown in Figure 15 and 16 respectively.

Compounding time was found to have a high influence on dispersion quality. Low compounding time (5 min) displayed poor dispersion and higher agglomeration of modified GO as shown in Figure 15(a) and 16(a). Figure 15(c) and 16(c) shows the 1 wt.% and 5 wt.% modified GO iPP nanocomposites compounded for 20 min respectively. The figures show the presence of agglomeration of modified GO in both cases. In perspective, the high compounding time (20 min) displayed some-how better dispersion than low compounding time (5 min). Intermediate compounding time (10 min) produced the best dispersion of modified GO in iPP nanocomposites as shown in Figure 15(b) and 16(b).

Increasing GO content from 1% to 5% resulted in a higher GO agglomeration. This shows that it was difficult to achieve a better dispersion as high filler loading. This phenomena found in this study agrees with many reported cases in literature [9].

Good dispersion of fillers in nanocomposites improves interaction of GO and matrix hence more bonds are formed resulting to enhanced physical properties. On the other hand, inadequate dispersion compromises interaction surfaces and the aggregates act as defects hence compromising properties of the nanocomposites [1].

Therefore, these results explain the high properties of tensile strength, Young's modulus and elongation at break at intermediate compounding time (10 min) for both 1 wt.% and 5 wt.% modified GO filled iPP nanocomposites.

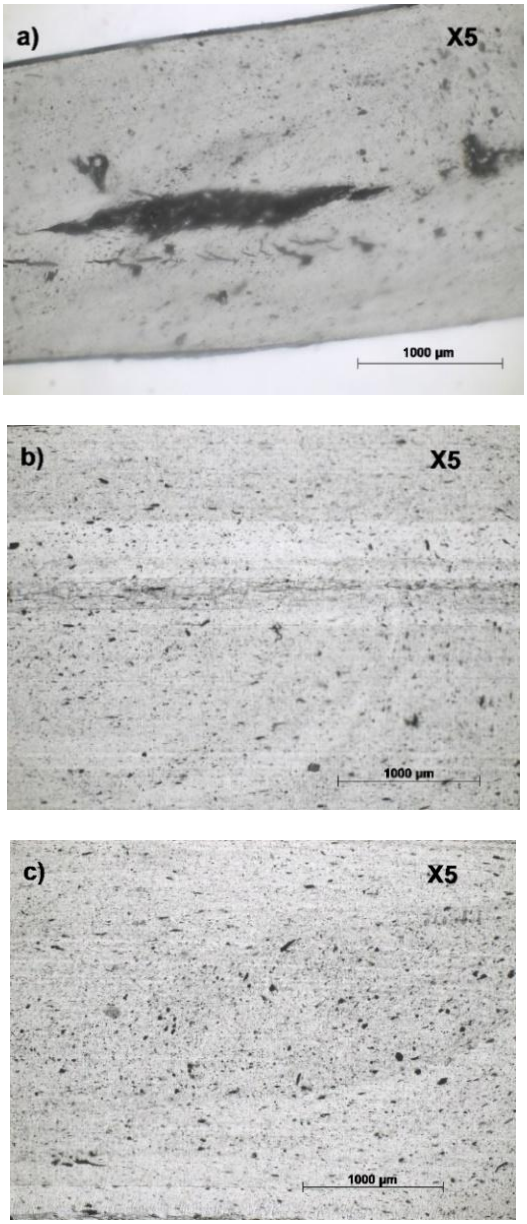

Figure 13: Dispersion micrographs of 1% GO filled iPP nanocomposites: (a) 5 min, (b) 10 min and (c) 20 min compounding time.

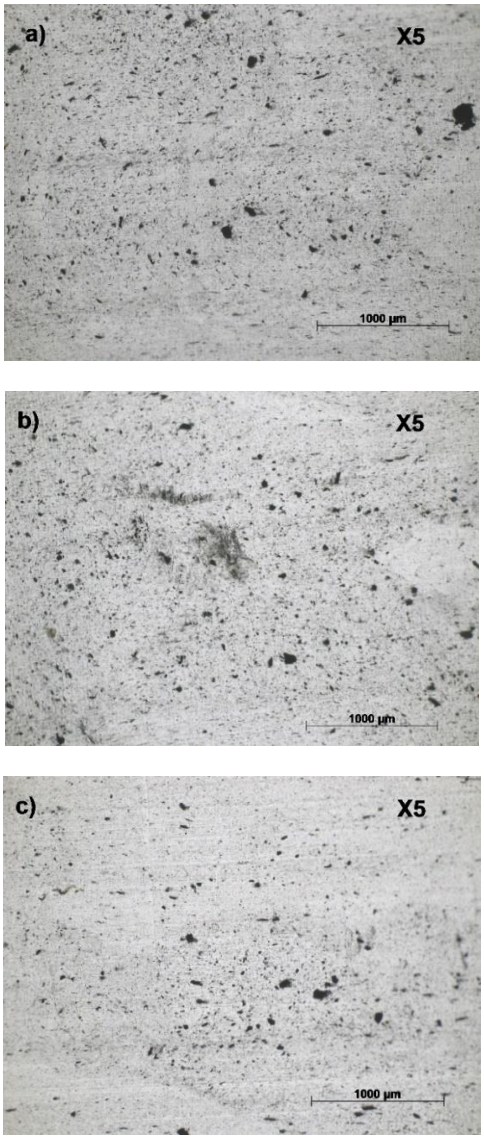

Figure 14: Dispersion micrographs of 5% GO filled iPP nanocomposites: (a) 5 min, (b) 10 min and (c) 20 min compounding time.

4. Conclusions

GO prepared using a modified Hummer's method was modified with ODA and then utilised in processing iPP nanocomposites through micro-compounding and injection molding. Investigated properties were found to be affected by modified GO content and compounding time. The factors investigated had different directional effects on mechanical properties of iPP nanocomposites. The iPP nanocomposites developed, had in-part enhanced mechanical properties in comparison to neat iPP.

Here-in, high filler iPP nanocomposites had higher tensile strength, elongation at break, storage modulus, loss modulus and crystallinity than low filler iPP nanocomposites. On the other hand, they had lower Young's modulus and toughness values than low filler iPP nanocomposites. A high filler iPP nanocomposite may be perceived to offer better performance although it shows poor dispersion and high rate of agglomeration as found in this study. Another pitfall is that higher filler nanocomposite will be costly in the production. Therefore, a balance of cost and properties of an iPP nanocomposite is a requirement in order to achieve optimum performance or properties.

Compounding time was found to influence nanocomposites properties greatly. Here-in, intermediate compounding time (10 min) resulted in more enhanced properties than the other compounding times. It resulted in higher tensile strength, Young's modulus, elongation at break and toughness in iPP nanocomposites. Intermediate compounding time iPP nanocomposites displayed better performance on essential mechanical properties than other compounding times. This may be attributed to the good dispersion and nil agglomeration as evidenced in light microscopy.

In general, the inferior mechanical enhancement properties found in this work can be attributed to lack of annealing of the specimens. Annealing is a heat treatment process that erases the thermal history of a material. It involves heating a material to a temperature above its recrystallization point, holding it for an appropriate time and finally cooling. This process increases the ductility of the material [32]. [Lin, Chen [31]] reported a remarkable increase in mechanical properties after annealing polypropylene/$CaCO_3$ nanocomposites. They reported annealed nanocomposites sustained fracture force of >200% than un-annealed samples, hence they required a higher force to initiate a crack. The fracture energy was therefore much larger in annealed nanocomposites, implying high toughness due to high energy absorption in the crack-initiation stage. Therefore, annealing is an important process to equilibrate the material after processing. This concern is supported by the DSC consistent results in this study. The results were acquired through a heat/cool/heat cycle, in order to erase the thermal history of the nanocomposite during the slow cooling cycle. Therefore, intermediate compounding time (10 min) iPP nanocomposites may be said to exhibit high interfacial interaction between polymer and filler, hence better mechanical properties.

5. Acknowledgment

This work was supported by Department of mechanical and manufacturing Engineering, Aalborg University, Denmark.

References

[1] Li, B. and W.-H. Zhong, Review on polymer/graphite nanoplatelet nanocomposites. Journal of Materials Science, 2011. 46(17): p. 5595-5614.
[2] Cho, D., et al., Dynamic Mechanical and Thermal Properties of Phenylethynyl-Terminated Polyimide Composites Reinforced With Expanded Graphite Nanoplatelets. Macromolecular materials and engineering, 2005. 290(3): p. 179-187.
[3] Geim, A.K. and K.S. Novoselov, The rise of graphene. Nature Materials, 2007. 6(3): p. 183-191.
[4] Potts, J.R., et al., Graphene-based polymer nanocomposites. Polymer, 2011. 52(1): p. 5-25.
[5] Paredes, J.I., et al., Graphene Oxide Dispersions in Organic Solvents. Langmuir, 2008. 24(19): p. 10560-4.

[6] Bellucci, F., et al., The Processing of Nanocomposites, in Dielectric Polymer Nanocomposites, J.K. Nelson, Editor. 2010, Springer US. p. 31--64.
[7] Li, W., et al., Simultaneous surface functionalization and reduction of graphene oxide with octadecylamine for electrically conductive polystyrene composites. Carbon, 2011. 49(14): p. 4724-4730.
[8] Schadler, L.S., Polymer-based and polymer-filled nanocomposites, in Nanocomposite Science and Technology, P.M. Ajayan, L.S. Schadler, and P.V. Braun, Editors. 2003, Wiley-VCH Verlag: Weinheim. p. 77-154.
[9] Gao, J., et al., Observation of strong nano- effect via tuning distributed architecture of graphene oxide in poly(propylene carbonate). Observation of strong nano-effect via tuning distributed architecture of graphene oxide in poly(propylene carbonate), 2014. 25(2): p. 025702.
[10] Bao, R.-Y.a.C., Jun and Liu, Zheng-Ying and Yang, Wei and Xie, Bang-Hu and Yang, Ming-Bo, Towards balanced strength and toughness improvement of isotactic polypropylene nanocomposites by surface functionalized graphene oxide. J. Mater. Chem. A, 2014. 2(9): p. 3190-3199.
[11] Wang, G., et al., Synthesis and characterisation of hydrophilic and organophilic graphene nanosheets. Carbon, 2009. 47(5): p. 1359-1364.
[12] Dimiev, A., et al., Pristine graphite oxide. Journal of the American Chemical Society, 2012. 134(5): p. 2815.
[13] Rosato, D.V., D.V. Rosato, and M.G. Rosato, Injection molding handbook / edited by Dominick V. Rosato, Donald V. Rosato, Marlene G. Rosato. 3. ed. ed, ed. D.V. Rosato. 2000: Boston, Mass. : Kluwer Academic.
[14] Salleh, M.A.M., The influences of melt-compounding parameters on the tensile properties of low filler loading of untreated-MWCNTs-polypropylene (PP) nanocomposites. Journal of Engineering Science and Technology, 2008. 3(1): p. 97-108.
[15] Wenig, W. and F. Herzog, Injection molding of polypropylene: X- ray investigation of the skin– core morphology. Journal of Applied Polymer Science, 1993. 50(12): p. 2163-2171.
[16] Eastman, Technical Data Sheet:Eastman G-3015 Polymer, Eastman, Editor. 2007.
[17] Borealis, Technical Data Sheet:Borealis HE365FB Polypropylene, Borealis, Editor. 2016.
[18] ISO, Plastics - Determination of tensile properties, in "DS EN ISO 527-5:2009 2009, Dansk Standard, Charlottenlund.
[19] ISO, Plastics - Determination of flexural properties, in DS EN ISO 178:2011. 2011, Dansk Standard, Charlottenlund.
[20] Sefadi, J., et al., Effect of surfactant and radiation treatment on the morphology and properties of PP/ EG composites. J Mater Sci, 2015. 50(18): p. 6021-6031.
[21] Carsalade, E., et al., Transitions/ relaxations in polyester adhesive/ PET system. J Therm Anal Calorim, 2010. 101(3): p. 849-857.
[22] ISO, Plastics - Determination of Izod impact strength, in DS EN ISO 180:2000 2000, Dansk Standard, Charlottenlund.
[23] Jang, J., et al., Dispersibility of reduced alkylamine-functionalized graphene oxides in organic solvents. J Colloid Interface Sci, 2014. 424.
[24] Qiu, F., et al., Functionalized graphene sheets filled isotactic polypropylene nanocomposites. Composites. Part B, Engineering, 2015. 71: p. 175-183.
[25] Jia, Y.U., et al., Creep and recovery of polypropylene/carbon nanotube composites. International journal of plasticity, 2011. 27(8): p. 1239-1251.
[26] Dorigato, A. and A. Pegoretti, Reprocessing effects on polypropylene/silica nanocomposites. Journal of applied polymer science, 2014. 131(10): p. n/a-n/a.
[27] Gregorova, A., Application of Differential Scanning Calorimetry to the Characterization of Biopolymers. 2013, InTech. p. 3-20.
[28] Bohnsack, K.M.a.D.A., Differential Scanning Calorimetry (DSC) as an Analytical Tool in Plastics Failure Analysis. 2013, TA Instruments.
[29] Yun, Y.S., et al., Reinforcing effects of adding alkylated graphene oxide to polypropylene. Carbon, 2011. 49(11): p. 3553-3559.
[30] Karian, P.D.H.G., Handbook of Polypropylene and Polypropylene Composites, ed. P.D.H.G. Karian. 1999: New York, NY, USA: CRC Press.
[31] Lin, Y., et al., High Impact Toughness Polypropylene/ CaCO3 Nanocomposites and the Toughening Mechanism. 2008. 41: p. 9204-9213.
[32] Coban, O., et al., The influence of annealing on the crystallization and tribological behavior of MWNT/PEEK nanocomposites. Polymer Composites, 2011. 32(11): p. 1766-1771.